GANIT

Available online at https://ganitjournal.bdmathsociety.org/

GANIT: Journal of Bangladesh Mathematical Society

GANIT *J. Bangladesh Math. Soc.* 45.1 (2025) 016–031
DOI: https://doi.org/10.3329/ganit.v45i1.80857

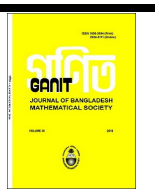

Backward Bifurcation Phenomena of Dengue Transmission in the Presence of Re-Infection and Imperfect Vaccine

Md. Mahfujur Rahman *[a], Chandra Nath Podder[b], and Amit Kumar Saha [c]

[a] *Department of Mathematics, Dhaka University of Engineering & Technology, Gazipur, Gazipur-1707, Bangladesh*
[b,c] *Department of Mathematics, University of Dhaka, Dhaka-1000, Bangladesh*

ABSTRACT

The transmission dynamics of the dengue disease with imperfect vaccination and re-infection are being considered & analyzed. The model exhibits backward bifurcation when the basic reproduction number ($\mathcal{R}_0$) is less than 1. However, using the Lyapunov function as well as the LaSalle Invariance Principle, it is demonstrated that with perfect vaccination and no re-infection, the DFE point is globally asymptotically stable. If $\mathcal{R}_0 > 1$, there exists a distinct endemic equilibrium that is locally asymptotically stable. Numerical results of the model, using relevant parameter values, indicate that the increasing rate of vaccination waning resulted in the increase of infected individuals. Further numerical results suggest that the disease will continue in the community in the presence of re-infection. It also suggests that the dengue virus can be controlled effectively using the perfect vaccine.

Received: February 17, 2025 **Accepted:** March 27, 2025 **Published Online:** June 30, 2025

Keywords: Dengue Virus; Vaccination; Re-Infection; Vaccination waning.

1 Introduction

Aedes mosquitoes can transmit the virus to human beings through their bite [1]. Almost all age groups, including infants and adults, are susceptible to dengue. Symptoms of dengue usually start to show 3–14 days after a mosquito bite [1]. The infected person is more likely to get dengue shock syndrome or dengue hemorrhagic fever 12 weeks later [2]. After recovering from one dengue serotype, a person gains lifetime immunity to that serotype but is still susceptible to the other three serotypes. In 2019, the world saw the highest number of cases ever reported. In the past 20 years, the number of cases has more than doubled, from 505, 430 in 2000 to over 2.4 million in 2010 and 5.2 million in 2019, according to WHO. Between 2000 and 2015, the overall number of deaths jumped from 960 to 4032 with the youngest age groups bearing the worst impact. In 2020 and 2021, the number of illnesses and deaths that are reported seems to be going down [1]. The dengue outbreak in Bangladesh is being prolonged by inadequate sanitation, improper hygiene systems and a dense population. To stop the spread of the disease, government representatives, non-governmental organizations, policymakers, and institutions must start taking quick nationwide action (e.g., mosquito control and vaccine deployment).

*Corresponding author. *E-mail address:* mahfujurrahman@duet.ac.bd

Therefore, the reduction of mosquitoes, through acts like larvaciding, adulticiding, and eliminating breeding grounds, as well as use of human protection (health care), are the primary strategies for preventing dengue transmission. Although research is ongoing, none of the four serotypes of the virus presently has a specific, effective human vaccination [1]. The potential effects of dengue vaccines are being evaluated using a variety of mathematical models that have been developed [3, 4, 5, 6]. Ferguson et al. [4] used a partial differential formulation that takes infection history into account to test the hypothesis that the Dengvaxia vaccine functions similarly to a hidden natural infection in increasing host immunity. According to research by Chao et al. [7], a vaccine with a 70% to 90% success rate has the potential to drastically decrease the frequency and severity in the short and medium term [8]. Gonzales-Morales et al. [8] demonstrated that vaccination programs can reduce the frequency and size of dengue outbreaks using mathematical modeling depending on vaccine interaction and dengue strain type. Backward bifurcation in the kinetics of dengue transmission was demonstrated by Garba et al.[3]. A fractional order model was suggested by Al-Sulami and Hamdan et al. [9, 10]. Also, Iboi and Gumel [11] mathematically evaluated the effectiveness of the vaccine immunization.
Here, we formulated a new model with imperfect vaccination and in the presence of re-infection in line with the model described in Garba et al. [3] by considering a compartment for the vaccinated infected human class and re-infection of the recovered human class. The model is formulated in section 2. The basic mathematical analysis and stability of the equilibrium points are presented in section 3. In section 4, numerical simulations and discussions are performed.

2 Model Formulation

The human individual is classified as: susceptible human(S_h), vaccinated human(B_h), exposed human (E_h), infected human(I_h), vaccinated infected human(I_{hb}), recovered human(R_h). So, the all population at time t is $N_h = S_h + B_h + E_h + I_h + I_{hb} + R_h$. Similarly, the vector population is classified as: susceptible mosquito(S_v), exposed mosquito(E_v), infected mosquito(I_v) and so, the total mosquito population is $N_v = S_v + E_v + I_v$.
We have considered the given assumptions in formulating the model:

A1: The susceptible individuals(S_h) are recruited into the human population at a constant rate Π_h.

A2: The susceptible mosquito population(S_v) is being produced at a constant rate Π_v.

A3: Exposed individuals are less infectious than infected individuals.

A4: Vaccinated infected individuals are less infectious than infected individuals.

The susceptible human population is generated via recruitment of humans (by birth or immigration) into the community (at a constant rate, Π_h). This population is decreased following infection which can be acquired via effective contact with an exposed or infectious vector at a rate λ_h (the force of infection of humans), given by

$$\lambda_h = \frac{C_{hv}\left(\eta_v E_v + I_v\right)}{N_h}, \tag{2.1}$$

where, $0 < \eta_v < 1$ represents the low transmissibility of the exposed mosquitoes compared to the infected mosquitoes.
Similarly, it can be shown that the force of infection of mosquitoes (denoted by λ_v), is given by

$$\lambda_v = \frac{C_{hv}\left(\eta_1 E_h + I_h + \eta_2 I_{hb}\right)}{N_h}, \tag{2.2}$$

here, $0 \leq \eta_1, \eta_2 < 1$ accounts for the relative infectiousness of exposed humans and vaccinated infected humans in relation to infected humans.
Now, we construct the following system of NDE to represent the transmission dynamics of the dengue virus while taking into account all of the assumptions:

$$
\begin{aligned}
\frac{dS_h}{dt} &= \Pi_h + \omega B_h - \zeta S_h - \lambda_h S_h - \mu_h S_h,\\
\frac{dB_h}{dt} &= \zeta S_h - \lambda_h(1-e)B_h - \omega B_h - \mu_h B_h,\\
\frac{dE_h}{dt} &= \lambda_h\left[S_h + (1-e)\,B_h + \alpha R_h\right] - \sigma_h E_h - \mu_h E_h,\\
\frac{dI_h}{dt} &= p\sigma_h E_h - \phi_h I_h - (\mu_h + \delta_h)\,I_h,\\
\frac{dI_{hb}}{dt} &= (1-p)\,\sigma_h E_h - \phi_{hb} I_h - (\mu_h + \delta_{hb})\,I_{hb},\\
\frac{dR_h}{dt} &= \phi_h I_h + \phi_{hb} I_{hb} - \mu_h R_h - \alpha\lambda_h R_h,\\
\frac{dS_v}{dt} &= \Pi_v - \lambda_v S_v - \mu_v S_v,\\
\frac{dE_v}{dt} &= \lambda_v S_v - \sigma_v E_v - \mu_v E_v,\\
\frac{dI_v}{dt} &= \sigma_v E_v - \mu_v I_v - \delta_v I_v.
\end{aligned}
\tag{2.3}
$$

Figure 2.1 illustrates the flow diagram of the model (2.3), while Table 2.1 describes the model's associated parameters.

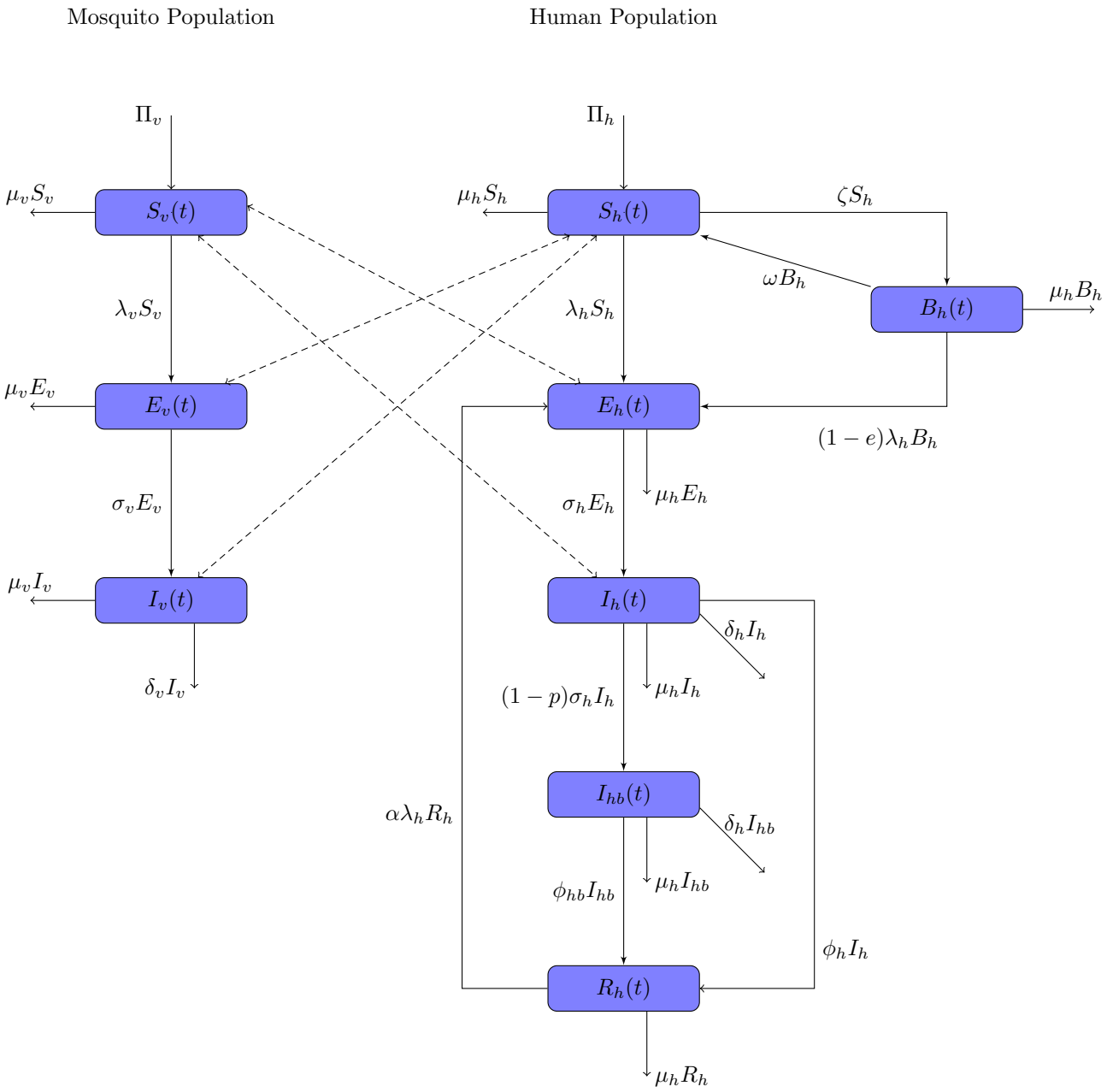

Figure 2.1: Model (2.3) flowchart.

Table 2.1: Model (2.3) parameters with descriptions.

Parameters	**Description**
Π_h	Recruitment rate of human
Π_v	Recruitment rate of mosquito
C_{hv}	Infection rate of mosquito
δ_h	Disease-induced death rate for human
δ_{hb}	Disease-induced death rate for vaccinated human
λ_h	The force of infection of human population
λ_v	The force of infection of mosquito population
μ_h	Natural death rates for human
μ_v	Natural death rate for mosquito
e	Vaccine efficacy
ζ	Vaccination rate
ω	Waning rate of vaccine
ϕ_h, ϕ_{hb}	Recovery rate
σ_h	Progression rate from E_h to I_h class
σ_v	Progression rate from E_v to I_v class
α, p, η_1, η_2, η_v	Modification parameters

3 Analysis of the Model

3.1 Positivity and boundedness of the model solutions

We have the following lemma:

Lemma 1. *The region,* $\Omega = \left\{\left(S_h,\, B_h,\, E_h,\, I_h,\, I_{hb},\, R_h,\, S_v,\, E_v,\, I_v\right) : S_h + B_h + E_h + I_h + I_{hb} + R_h \leq \dfrac{\Pi_h}{\mu_h},\, S_v + E_v + I_v \leq \dfrac{\Pi_v}{\mu_v}\right\} \subset \mathbb{R}^9_+$, *is positively invariant and attracting for the fundamental model (2.3).*

The lemma can be proved using the procedure described in [12].

3.2 Disease-free equilibrium(DFE)

The DFE of the model (2.3) is given by

$$\begin{aligned} E_0 &= \left(S_h^*,\, B_h^*,\, E_h^*,\, I_h^*,\, I_{hb}^*,\, R_h^*,\, S_v^*,\, E_v^*,\, I_v^*\right), \\ &= \left(\frac{\Pi_h\left(\omega+\mu_h\right)}{\mu_h\left(\zeta+\omega+\mu_h\right)},\, \frac{\Pi_h\zeta}{\mu_h\left(\zeta+\omega+\mu_h\right)}, 0,\, 0\, 0,\, 0,\, \frac{\Pi_v}{\mu_v},\, 0,\, 0\right). \end{aligned}$$

3.3 Local Stability of DFE

The transmission matrix F (associated with new infection terms) and the transition matrix V (considering transferred terms) are calculated using the idea in [13, 14] and are given by

$$F = \begin{bmatrix} 0 & 0 & 0 & C_{hv}\eta_v k_8 & C_{hv}k_8 \\ 0 & 0 & 0 & 0 & 0 \\ 0 & 0 & 0 & 0 & 0 \\ \dfrac{C_{hv}\eta_1\Pi_v\mu_h}{\mu_v\Pi_h} & \dfrac{C_{hv}\Pi_v\mu_h}{\mu_v\Pi_h} & \dfrac{C_{hv}\eta_2\Pi_v\mu_h}{\mu_v\Pi_h} & 0 & 0 \\ 0 & 0 & 0 & 0 & 0 \end{bmatrix},$$

and

$$V = \begin{bmatrix} k_1 & 0 & 0 & 0 & 0 \\ -p\sigma_h & k_2 & 0 & 0 & 0 \\ -(1-p)\,\sigma_h & 0 & k_3 & 0 & 0 \\ 0 & 0 & 0 & k_4 & 0 \\ 0 & 0 & 0 & -\sigma_v & k_5 \end{bmatrix},$$

where, $k_1 = \sigma_h + \mu_h$, $k_2 = \phi_h + \mu_h + \delta_h$, $k_3 = \phi_{hb} + \mu_h + \delta_{hb}$, $k_4 = \sigma_v + \delta_v$, $k_5 = \mu_v + \delta_v$. Therefore, $\mathcal{R}_0$ is expressed as

$$\mathcal{R}_0 = \frac{C_{hv}\sqrt{-k_1k_2k_3k_4k_5\mu_v\Pi_h\mu_h\Pi_v k_8\left(\eta_v k_5 + \sigma_v\right)\left[\eta_2 k_2\left(-1+p\right)\sigma_h - \eta_1 k_2 k_3 - p\sigma_h k_3\right]}}{k_1k_2k_3k_4k_5\mu_v\Pi_h}. \tag{3.1}$$

Theorem 1. *The DFE, E_0, of the model (2.3) is locally asymptotically stable if $\mathcal{R}_0 < 1$ and unstable if $\mathcal{R}_0 > 1$.*

3.4 Effect of Perfect Vaccination and No re-infection

3.4.1 Global stability of the DFE in the case of perfect vaccination ($\omega = 0$) and no re-infection ($\alpha = 0$)

Theorem 2. *When $\mathcal{R}_0 < 1$, the DFE, E_0, is globally asymptotically stable.*

Proof. Let the Lyapunov function

$$\mathcal{F} = f_1E_h + f_2I_h + f_3I_{hb} + f_4E_v + f_5I_v, \tag{3.2}$$

where,

$$\begin{aligned}
A &= \sqrt{-k_1k_2k_3k_4k_5k_8\mu_h\mu_v\Pi_h\Pi_v\left(\eta_v k_5 + \sigma_v\right)\left[\eta_2 k_2\left(-1+p\right)\sigma_h - \eta_1 k_2 k_3 - p\sigma_h k_3\right]},\\
B &= p\eta_2 k_2\sigma_h - pk_3\sigma_h - \eta_1 k_2 k_3 - \eta_2 k_2\sigma_h,\\
f_1 &= -\frac{\Pi_v\mu_h k_5 B\left(\eta_v k_5 + \sigma_v\right)}{A},\\
f_2 &= \frac{\Pi_v\mu_h\left(\eta_v k_5 + \sigma_v\right)k_1k_3k_5}{A},\\
f_3 &= \frac{\eta_2\Pi_v\mu_h\left(\eta_v k_5 + \sigma_v\right)k_1k_2k_5}{A},\\
f_4 &= \frac{\eta_v k_5 + \sigma_v}{k_4},\\
f_5 &= 1.
\end{aligned}$$

Now, from (3.2) we have

$$\begin{aligned}
\dot{\mathcal{F}} &= f_1\dot{E}_h + f_2\dot{I}_h + f_3\dot{I}_{hb} + f_4\dot{E}_v + f_5\dot{I}_v,\\
&= -\frac{\Pi_v\mu_h k_5 B\left(\eta_v k_5 + \sigma_v\right)}{A}\left[\lambda_h\left(S_h^* + (1-e)\,B_h^*\right) - k_1E_h\right] + \frac{\Pi_v\mu_h k_1k_3k_5\left(\eta_v k_5 + \sigma_v\right)}{A}\left[p\sigma_h E_h - k_2I_h\right]\\
&+ \frac{\eta_2\Pi_v\mu_h\left(\eta_v k_5 + \sigma_v\right)k_1k_2k_5}{A}\left[(1-p)\,\sigma_h E_h - k_3I_{hb}\right] + \frac{\eta_v k_5 + \sigma_v}{k_4}\left[\frac{\lambda_v\Pi_v}{\mu_v} - k_4E_v\right] + \sigma_v E_v - k_5I_v,\\
&= \left(\eta_v k_5 + \sigma_v\right)\Pi_v C_{hv}\mu_h\left[\frac{\eta_1 E_h}{k_4\Pi_h\mu_v\mathcal{R}_0} + \frac{I_h}{\Pi_h\mu_v k_4\mathcal{R}_0} + \frac{\eta_2 I_{hb}}{k_4\Pi_h\mu_v\mathcal{R}_0} + \frac{k_5B\eta_v k_8E_v}{A} + \frac{Bk_5k_8I_v}{A}\right]\left(\mathcal{R}_0 - 1\right).
\end{aligned}$$

Thus, $\dot{\mathcal{F}} < 0$ if $\mathcal{R}_0 < 1$ and $\dot{\mathcal{F}} = 0$ if and only if $\dot{E}_h = \dot{I}_h = \dot{I}_{hb} = \dot{E}_v = \dot{I}_v = 0$. According to the LaSalle Invariance Principle [15], the DFE, E_0, is globally asymptotic stable if $\mathcal{R}_0 \leq 1$. □

3.5 Stability of Endemic Equilibrium

Let the endemic equilibrium point be

$$E_1 = \left(S_h^{**},\, B_h^{**},\, E_h^{**},\, I_h^{**},\, I_{hb}^{**}, R_h^{**},\, S_v^{**},\, E_v^{**},\, I_v^{**}\right),$$

where

$$
\begin{aligned}
S_h^{**} &= \frac{\Pi_h\left(\lambda_h^{**}(1-e)+\omega+\mu_h\right)}{\left(\zeta+\mu_h+\lambda_h^{**}\right)\left[\lambda_h^{**}(1-e)+\omega+\mu_h\right]-\omega\zeta},\\
B_h^{**} &= \frac{\zeta\Pi_h}{\left(\zeta+\mu_h+\lambda_h^{**}\right)\left[\lambda_h^{**}(1-e)+\omega+\mu_h\right]-\omega\zeta},\\
E_h^{**} &= \frac{\lambda_h^{**}\Pi_h\left[\lambda_h^{**}(1-e)+k_6+\zeta(1-e)\right]\left(\mu_h+\alpha\lambda_h^{**}\right)}{k_1\left[\left(\zeta+\mu_h+\lambda_h^{**}\right)\left(\lambda_h^{**}(1-e)+k_6\right)-A_3\right]\left(\mu_h+\alpha\lambda_h^{**}-A_2\lambda_h^{**}\right)},\\
I_h^{**} &= \frac{p\sigma_h\lambda_h^{**}\Pi_h\left[\lambda_h^{**}(1-e)+k_6+\zeta(1-e)\right]\left[\mu_h+\alpha\lambda_h^{**}\right]}{k_1k_2\left[\left(\zeta+\mu_h+\lambda_h^{**}\right)\left(\lambda_h^{**}(1-e)+k_6\right)-A_3\right]\left(\mu_h+\alpha\lambda_h^{*}-A_2\lambda_h^{**}\right)},\\
I_{hb}^{**} &= \frac{\lambda_h^{**}\Pi_h\sigma_h\left[\lambda_h^{**}(1-e)+k_6+\zeta(1-e)\right]\left(\mu_h+\alpha\lambda_h^{**}\right)(1-p)}{k_1k_3\left[\left(\zeta+\mu_h+\lambda_h^{**}\right)\left(\lambda_h^{**}(1-e)+k_6\right)-A_3\right]\left(\mu_h+\alpha\lambda_h^{**}-A_2\lambda_h^{**}\right)},\\
R_h^{**} &= \frac{\lambda_h^{**}\Pi_hA_1\left[\lambda_h^{**}(1-e)+k_6+\zeta(1-e)\right]}{k_1\left[\left(\zeta+\mu_h+\lambda_h^{**}\right)\left(\lambda_h^{**}(1-e)+k_6\right)-A_3\right]\left(\mu_h+\alpha\lambda_h^{**}-A_2\lambda_h^{**}\right)},\\
S_v^{**} &= \frac{\Pi_v}{\lambda_v^{**}+\mu_v},\\
E_v^{**} &= \frac{\Pi_v\Pi_v}{k_4\left(\lambda_v^{**}+\mu_v\right)},\\
I_v^{**} &= \frac{\sigma_v\Pi_v\Pi_v}{k_4k_5\left(\lambda_v^{**}+\mu_v\right)}.
\end{aligned}
\tag{3.3}
$$

At the endemic equilibrium state, the forces of infection (with mass action) are

$$
\lambda_h^{**}=C_{hv}\left(\eta_vE_v^{**}+I_v^{**}\right);\qquad \lambda_v^{**}=C_{hv}\left(\eta_1E_h^{**}+I_h^{**}+\eta_2I_{hb}^{**}\right). \tag{3.4}
$$

Using (3.3) in (3.4),we obtain

$$
\lambda_h^{**}\left[A_{18}(\lambda_h^{**})^3+A_{22}(\lambda_h^{**})^2+A_{23}\lambda_h^{**}+A_{24}\right]=0, \tag{3.5}
$$

where,

$$
\begin{aligned}
A_{18} &= \alpha(1-e)C_{hv}\Pi_h\left[\eta_1+\frac{p\sigma_h}{k_2}+\frac{\eta_2(1-p)\sigma_h}{k_3}\right]+\alpha(1-e)k_1\left[1-\frac{\left(p\phi_hk_3+k_2(1-p)\phi_{hb}\right)\sigma_h}{k_1k_2k_3}\right],\\
A_{22} &= C_{hv}\Pi_h\left(\eta_1+\frac{p\sigma_h}{k_2}+\frac{\eta_2(1-p)\sigma_h}{k_3}\right)\left[\mu_h(1-e)+\alpha k_6+\alpha(1-e)\zeta-\frac{\alpha(1-e)C_{hv}\Pi_v\left[\eta_v+\frac{\sigma_v}{k_5}\right]}{k_4}\right]\\
&\quad+\mu_vk_1\mu_h(1-e)+\mu_v\alpha k_1\left[1-\frac{\sigma_h\left(p\phi_hk_3+k_2(1-p)\phi_{hb}\right)}{k_1k_2k_3}\right]\left[\zeta(1-e)+k_6+\mu_h(1-e)\right],\\
A_{23} &= C_{hv}\mu_h\Pi_h\left[\eta_1+\frac{p\sigma_h}{k_2}+\frac{\eta_2(1-p)\sigma_h}{k_3}\right]\left(k_6+(1-e)\zeta\right)+\mu_v\alpha k_1\left[1-\frac{\sigma_h\left(p\phi_hk_3+k_2(1-p)\phi_{hb}\right)}{k_1k_2k_3}\right]\\
&\quad-\frac{\left(\eta_v+\frac{\sigma_v}{k_5}\right)(1-e)\mu_h\Pi_h\Pi_vC_{hv}^2\left[\eta_1+\frac{p\sigma_h}{k_2}+\frac{(1-p)\eta_2\sigma_h}{k_3}\right]}{k_4}+\mu_vk_1\mu_h\Big((1-e)\zeta+k_6+(1-e)\mu_h\Big)\\
&\quad\Big(\zeta k_6+\mu_hk_6-\omega\zeta\Big),\\
A_{24} &= \mu_v\mu_h^2k_1\Big(\zeta+\omega+\mu_h\Big)\Big[1-\mathcal{R}_d^2\Big].
\end{aligned}
$$

The root $\lambda_h^{**}=0$ of (3.5) corresponds to the DFE and other non-zero equilibria satisfy the following equation.

$$
f(\lambda^{**})=A_{18}(\lambda_h^{**})^3+A_{22}(\lambda_h^{**})^2+A_{23}\lambda_h^{**}+A_{24}, \tag{3.6}
$$

Backward bifurcation may occur if there are several non-zero (endemic) equilibria. The coefficient A_{18} is always positive, but A_{24} is positive if $\mathcal{R}_d$ is less than one and negative if $\mathcal{R}_d$ is more than one, as can be seen from the above. Hence we have the following results using [12].

Case-1: For $\mathcal{R}_d^2 > 1$

Table 3.1: Depending on the sign of Δ, A_{22}, and A_{23}, number of real positive roots

Δ	A_{22}	A_{23}	No. of real positive roots of $f(\lambda^{**})$
> 0	> 0	< 0	1
> 0	> 0	> 0	1
> 0	< 0	< 0	1
> 0	< 0	> 0	1 if $f(\lambda_-^{**}) < 0$ and 3 if $f(\lambda_-^{**}) > 0$

Case-2: For $\mathcal{R}_d^2 < 1$

Table 3.2: Depending on the sign of Δ, A_{22}, and A_{23}, number of real positive roots

Δ	A_{22}	A_{23}	No. of real positive roots of $f(\lambda^{**})$
> 0	> 0	> 0	0
> 0	< 0	> 0	0
> 0	< 0	< 0	2
> 0	< 0	> 0	0 if $f(\lambda_+^{**}) > 0$ and 2 if $f(\lambda_-^{**}) < 0$

By Table 3.2, we can observe that two endemic equilibria exist. So when $A_{22} < 0$ and $A_{23} < 0$, a phenomena of backward bifurcation may occur.

3.6 Presence of Backward Bifurcation

We apply the centre manifold theory [13, 16] investigating the possibilities of backward bifurcation. For this, we use change of variables. Let $S_h = x_1, B_h = x_2, E_h = x_3, I_h = x_4, I_{hb} = x_5, R_h = x_6, S_v = x_7, E_v = x_8, I_v = x_9$, such that $N_h = x_1 + x_2 + x_3 + x_4 + x_5 + x_6$ and $N_v = x_7 + x_8 + x_9$. Here, the Jacobian of the system at the DFE (E_1), denoted by $J(E_1)$, is given by

$$J(E_1) = \begin{pmatrix} -\zeta - \mu_h & \omega & 0 & 0 & 0 & 0 & 0 & -\eta_v j_1 & -j_1 \\ \zeta & -\omega - \mu_h & 0 & 0 & 0 & 0 & 0 & \eta_v j_2 & j_2 \\ 0 & 0 & -k_1 & 0 & 0 & 0 & 0 & -\eta_v j_3 & -j_3 \\ 0 & 0 & p\sigma_h & -k_2 & 0 & 0 & 0 & 0 & 0 \\ 0 & 0 & -(p-1)\sigma_h & 0 & -k_3 & 0 & 0 & 0 & 0 \\ 0 & 0 & 0 & \phi_h & \phi_{hb} & -\mu_h & 0 & 0 & 0 \\ 0 & 0 & -\eta_1 j_4 & -j_4 & -\eta_2 j_4 & 0 & -\mu_v & 0 & 0 \\ 0 & 0 & \eta_1 j_4 & j_4 & \eta_2 j_4 & 0 & 0 & -k_4 & 0 \\ 0 & 0 & 0 & 0 & 0 & 0 & 0 & \sigma_v & -k_5 \end{pmatrix},$$

where,

$$k_1 = \sigma_h + \mu_h, \qquad k_2 = \phi_h + \mu_h + \delta_h, \qquad k_3 = \phi_{hb} + \mu_h + \delta_{hb}, \qquad k_5 = \mu_v + \delta_v,$$

$$k_6 = \mu_h + \omega, \qquad k_7 = \frac{\Pi_h}{\mu_h\left(\mu_h + \omega + \zeta\right)}, \qquad k_8 = \frac{\mu_h + \omega + \zeta\left(1 - e\right)}{\mu_h + \omega + \zeta}, \qquad g = \left(1 - e\right),$$

$$j_1 = \frac{C_{hv}(\mu_h+\omega)}{\mu_h+\omega+\zeta}, \qquad j_2 = \frac{\zeta(e-1)C_{hv}}{\mu_h+\omega+\zeta}, \qquad j_3 = \frac{C_{hv}(e\zeta-\zeta-\omega-\mu_h)}{\mu_h+\omega+\zeta}, \qquad j_4 = \frac{\Pi_v\mu_h C_{hv}}{\mu_v\Pi_h}.$$

When $\mathcal{R}_0 = 1$, we have from (3.1)

$$\beta = \frac{k_1k_2k_3k_4k_5\mu_v\Pi_h}{\sqrt{-k_1k_2k_3k_4k_5\mu_v\Pi_h\mu_h\Pi_v k_8\left(\eta_v k_5+\sigma_v\right)\left[\eta_2k_2\left(-1+p\right)\sigma_h-\eta_1k_2k_3-p\sigma_hk_3\right]}}. \tag{3.7}$$

Simple eigenvalues of zero exist in the Jacobian $(J(E_1))$ (with all other eigenvalues having negative real part). The dynamics of the model can therefore be examined using the central manifold theory [16, 17].

Eigenvectors of $J_\beta = J(E_1)$: For $\mathcal{R}_0 = 1$, the Jacobian denoted by (J_β) at β has a right eigenvector with the zero eigenvalues which is given by $w = (w_1,\, w_2,\, w_3,\, w_4,\, w_5,\, w_6,\, w_7,\, w_8,\, w_9,)^T$, where,

$$w_1 = 1, \qquad w_4 = \frac{p\sigma_h w_3}{k_2}, \qquad w_7 = -\frac{\eta_1 j_4 w_3 + j_4 w_4 + \eta_2 j_4 w_5}{\mu_v},$$
$$w_2 = \frac{\zeta w_1 + \eta_v j_2 w_8 + j_2 w_9}{\omega+\mu_h}, \qquad w_5 = \frac{w_3\sigma_h\left(1-p\right)}{k_3}, \qquad w_8 = \frac{\eta_1 j_4 w_3 + j_4 w_4 + \eta_2 j_4 w_5}{k_4},$$
$$w_3 = 1, \qquad w_6 = \frac{\phi_h w_4 + \phi_{hb} w_5}{\mu_h}, \qquad w_9 = \frac{\sigma_v w_8}{k_5}.$$

Moreover, The left eigenvector of J_β is given by $v = [v_1,\, v_2,\, v_3,\, v_4,\, v_5,\, v_6,\, v_7,\, v_8,\, v_9]$, where,

$$v_1 = 1, \qquad v_4 = \frac{j_4 v_8}{k_2}, \qquad v_7 = 0,$$
$$v_2 = \frac{v_1\left(\zeta+\mu_h\right)}{\zeta}, \qquad v_5 = \frac{\eta_2 j_4 v_8}{k_3}, \qquad v_8 = 1,$$
$$v_3 = \frac{p\sigma_h v_4 + v_5\sigma_h\left(1-p\right) + \eta_1 j_4 w_8}{k_1}, \qquad v_6 = 0, \qquad v_9 = \frac{\eta_v j_1 v_1 - \eta_v j_2 v_2 + \eta_v j_3 v_3 + k_4 v_8}{\sigma_v}.$$

Computation of a **&** b**:**

The expression for a is after some calculation

$$a = \frac{1}{k_7^2(\zeta+k_6)^2\mu_v} \times \Big[2 \times ((((\eta_v w_8 + w_9)(gw_2 - w_3 - w_4 - w_5 + (\alpha-1)w_6 - w_2)y_3$$
$$- (gy_2w_2 - y_1(w_5+w_6+w_2+w_3+w_4))w_8\eta_v + (-gy_2w_2 + y_1(w_5+w_6+w_2+w_3+w_4))w_9$$
$$+ w_7y_8(\eta_1w_3 + \eta 2w_5 + w_4))k_6 + (-(\eta_v w_8 + w_9)((w_5+w_6+w_1+w_3+w_4)g - w_6\alpha - w_1)y_3$$
$$+ w_8(y_2(w_5+w_6+w_1+w_3+w4)g - y_1w_1)\eta_v + (y_2(w_5+w_6+w_1+w_3+w_4)g - y_1w_1)w_9 +$$
$$w_7y_8(\eta_1w_3 + \eta 2w5 + w4))\zeta)k_7\mu_v - y_8\Pi_v(\eta_1w_3 + \eta_2w_5 + w_4)(w_5+w_6+w_1+w_2+w_3+w_4)))C_{hv})\Big]$$

and the expression for b is

$$b = \frac{1}{k_7(\zeta+k_6)\mu_v} \times \Big(\zeta g\eta_v k_7\mu_v w_8y_2 - \zeta g\eta_v k_7\mu_v w_8y_3 - \zeta g k_7\mu_v w_9y_3 + \eta_v k_6k_7\mu_v w_8y_1 - \eta_v k_6k_7\mu_v w_8y_3$$
$$+ y_2w_9k_6k_7\mu_v - k_6k_7\mu_v w_9y_3 - \Pi_v\eta_1w_3y_8 - \Pi_v\eta_2w_5y_8 - \Pi_v w_4y_8\Big),$$
$$> 0.$$

Here, the sign of a is not known. So we have to put conditions on a to exist backward bifurcation. Hence, at $\mathcal{R}_0 = 1$ whenever $a > 0$, the model (2.3) undergoes backward bifurcation. We have some theorems. This are:

Theorem 3. *If the condition* $a > 0$ *is true, the model (2.3) exhibits backward bifurcation at* $\mathcal{R}_0 = 1$.

4 Numerical Simulations and Discussions

The analytical results are interpreted by simulating the model (2.3) with various parameter values from Table 4.1 in this section. The phenomenon of backward bifurcation, in which a stable endemic equilibrium coexists with a stable disease-free equilibrium, is depicted graphically in Figure 4.1. The trajectories of the model solution are shown in Figure 4.2 whenever $\mathcal{R}_0 < 1$. According to this figure, the disease will be eliminated from the community since the solution trajectory trends toward the DFE. Figure 4.3 depicts that when $\mathcal{R}_0 > 1$, the solution trajectories converge to endemic equilibrium and in this case, the disease will continue to spread throughout the community. Figure 4.4 shows that if vaccine efficacy(e) increases, the number of infected humans decreases. The epidemiological significance is that the disease can be controlled effectively by increasing the vaccine efficacy. This figure demonstrates that by increasing the vaccine efficacy from 50% to 75%, the peak of daily infected humans decreases by 15%. Further, Figure 4.5 demonstrates that if the vaccine waning rate is increased, the number of infected humans also increases. For example, when the waning rate of the vaccine increases from 50% to 75%, the peak of daily infected humans increases by 23%. Figure 4.6 illustrates that if the re-infection rate increases, the number of infected individuals increases. From figure 4.7, we observe that if the vaccination rate is increased, the infected number of humans can be decreased. This figure illustrates that when the vaccination rate increases from 50% to 80%, the peak of daily infected cases decreases by 8%. The figure 4.8 demonstrates that increasing the modification parameter η_1 correlates with reducing the number of infected individuals.

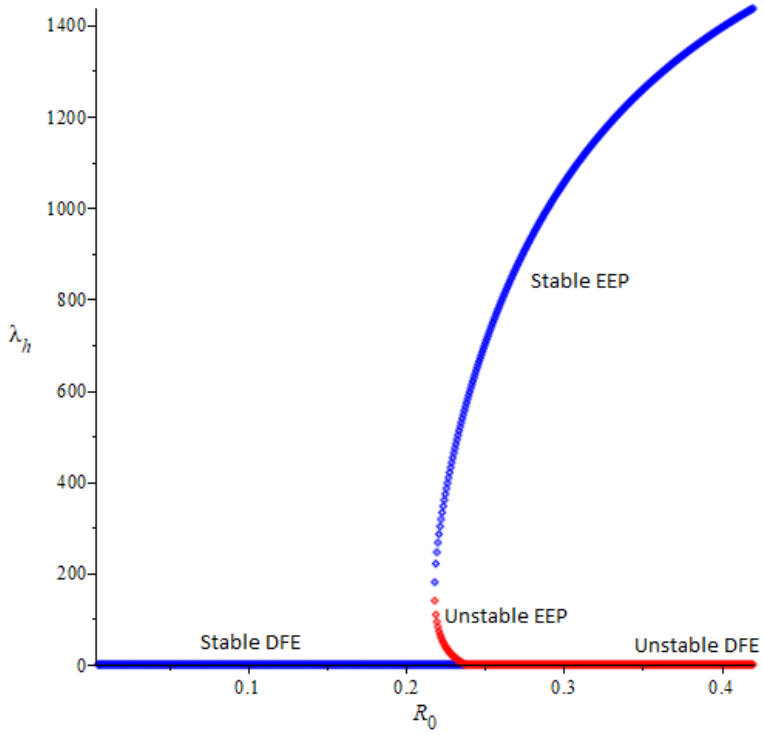

Figure 4.1: Backward bifurcation diagram of the model (2.3) using: $p = .5$, $\alpha = 10$, $e = .92$, $\omega = 10.9$, $\mu_h = 0.195e - 1$, $\mu_v = 0.16e - 1$, $\delta_h = .19$, $\delta_v = 0.57e - 1$, $\delta_{hb} = .28$, $\phi_h = .21$, $\phi_{hb} = .2$, $\sigma_h = 0.46e - 1$, $\sigma_v = 0.46e - 1$, $\eta_1 = .1$, $\eta_2 = .2$, $\eta_v = 0.7e - 1$, $\Pi_h = 100$, $\Pi_v = 120$, $C_{hv} = .15$, $\zeta = 14.9$. (so that $a > 0$ and $b > 0$).

Figure 4.1 graphically illustrates the phenomenon of backward bifurcation, which is characterized by the coexistence of a stable endemic equilibrium and a stable disease-free equilibrium.

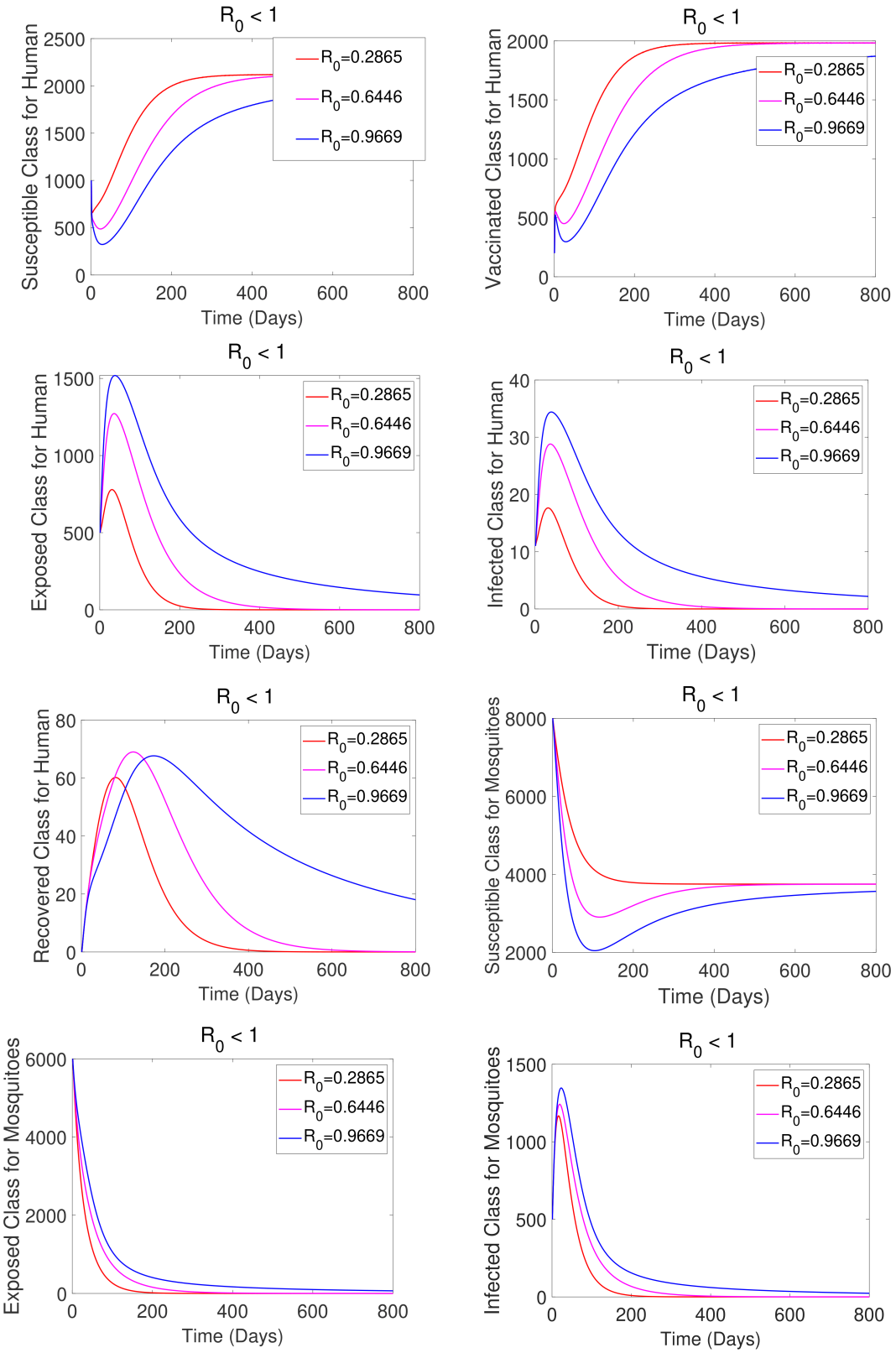

Figure 4.2: When $\mathcal{R}_0 < 1$, the solution of the model (2.3) indicates that the solution trajectory goes to DFE.

When $\mathcal{R}_0$ is less than 1, Figure 4.2 displays the model solution's trajectories. This figure shows that as the solution trajectory is trending toward the DFE, the disease will be eradicated from the community. From this

figure, we obtain that with the increasing basic reproduction number, the infected classes and exposed classes are increasing. At the same time, with the increasing basic reproduction number, the susceptible classes, recovered classes, and vaccinated classes are decreasing.

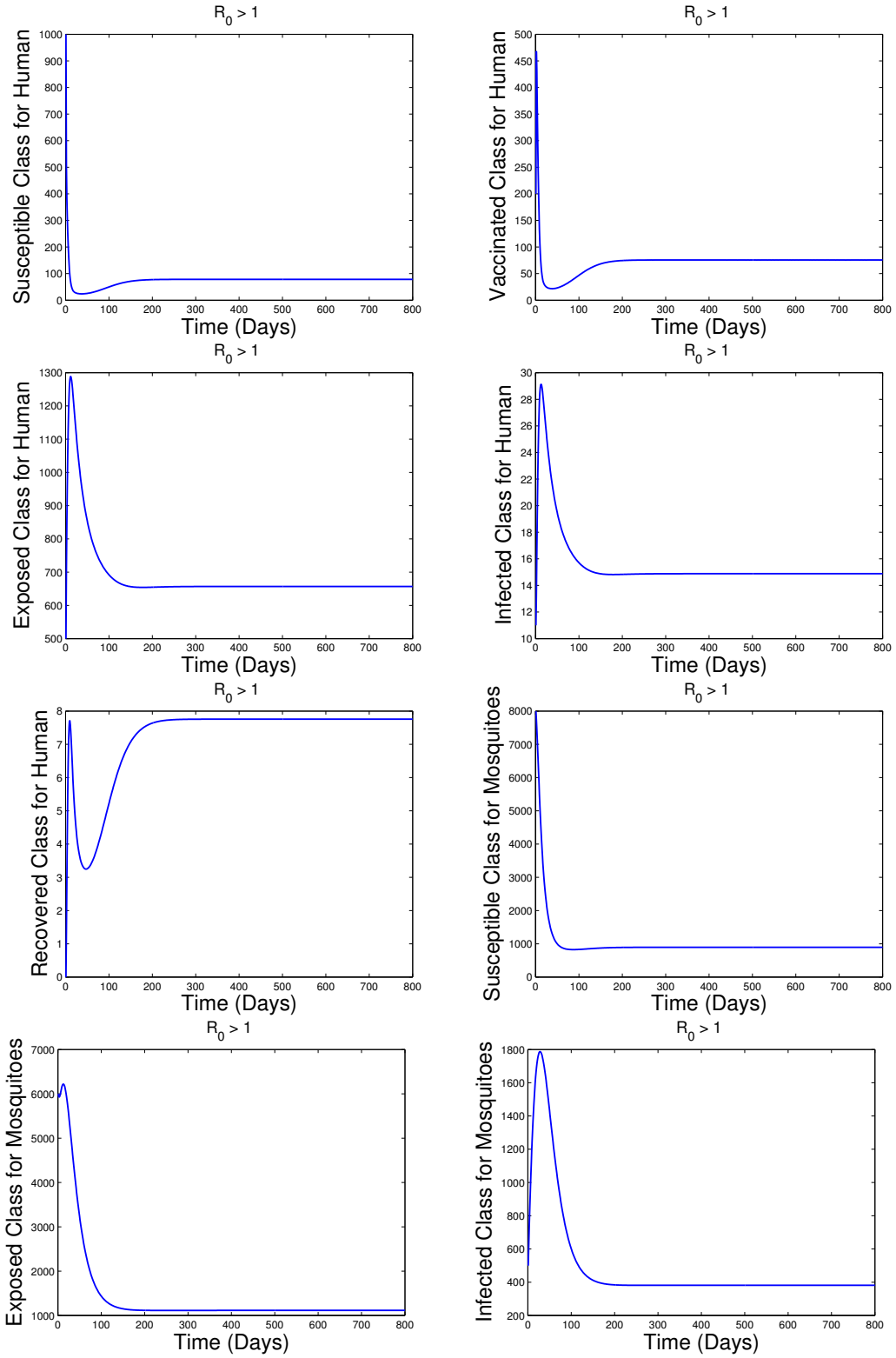

Figure 4.3: When $\mathcal{R}_0 > 1$, solution of the model (2.3) shows that the solution trajectory tends to EE. The parameter values listed in Table 4.1 were used with $\delta_h = 0.99, \Pi_h = 30, \Pi_v = 60, C_{hv} = 0.58, \zeta = 0.96$.

The solution trajectories converge to endemic equilibrium when $\mathcal{R}_0 > 1$, as seen in Figure 4.3, and then the disease continues to spread across the community.

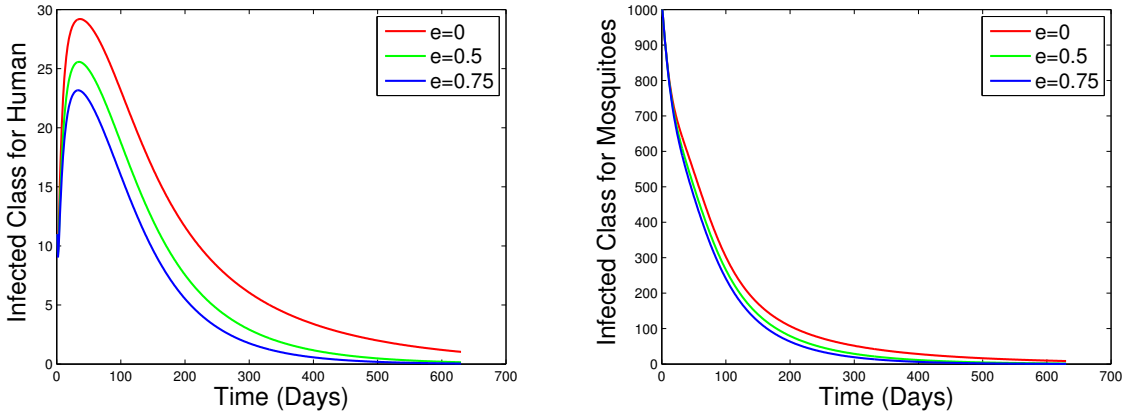

Figure 4.4: The impact of vaccine efficacy(e) is demonstrated using model simulations.

Figure 4.4 represents the effects of vaccine efficacy(e) for a 700 days timeline. If we do not use the vaccine, the number of infected classes both humans and mosquitoes is highest, and the red curve represents this number when vaccine efficacy is 0.5 then the number of infected classes is shown by the green curve. When the vaccine efficacy is 0.75, the blue curve represents the number of infected classes.

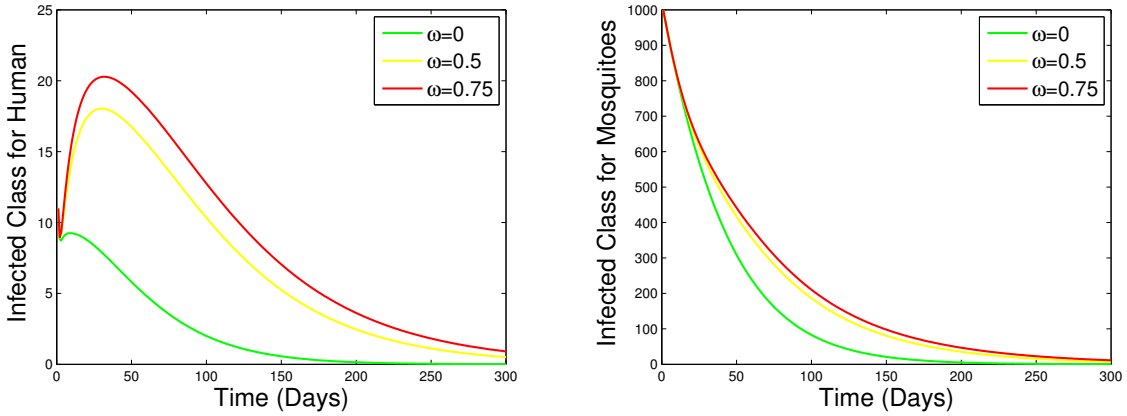

Figure 4.5: The impact of waning rate of vaccine(ω) is demonstrated using model simulations.

Figure 4.5 shows the effects of the waning rate of the vaccine(ω) . Our model gives the same assumption as the real-world situation.

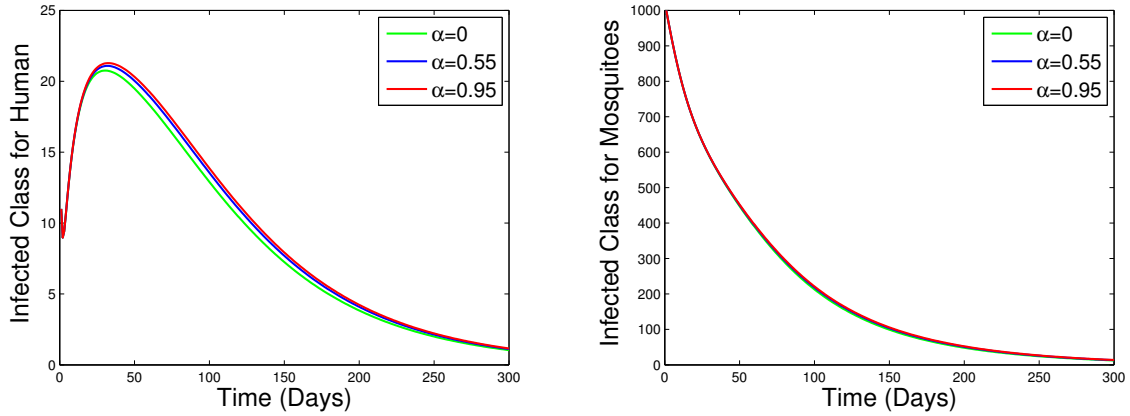

Figure 4.6: The impact of re-infection(α) is demonstrated using model simulations.

Figure 4.6 represents that with the increase of re-infection, the number of infected classes is increasing.

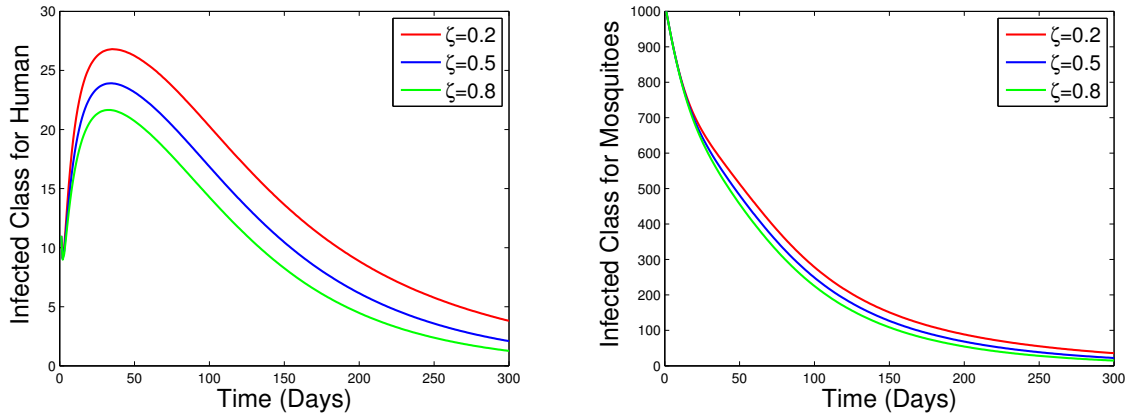

Figure 4.7: The impact of vaccination rate(ζ) is demonstrated using model simulations.

Figure 4.7 shows that with the increase of vaccination rate(ζ) , the number of infected classes also increases. It gives the same situation as the real world.

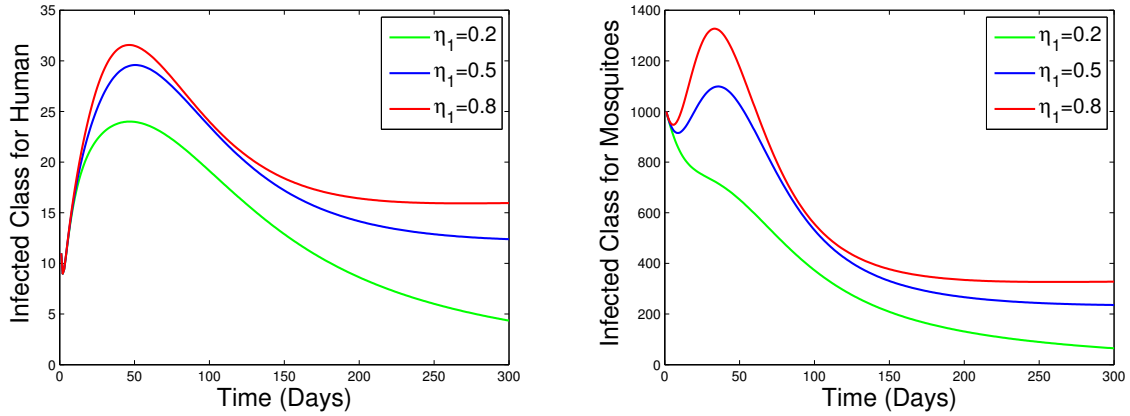

Figure 4.8: The impact of modification parameter(η_1) is demonstrated using model simulations.

From Figure 4.8, the modification parameter(η_1) is related to the exposed class. When (η_1) is increasing, the exposed class is also increasing. Figure 4.8 shows the scenario for this case.

Table 4.1: Parameter values of the model (2.3) for simulation.

Parameters	Nominal value	References
Π_h	80	[3]
Π_v	60	[3]
μ_h	0.0195	[3]
μ_v	0.016	[3]
δ_h	0.1	assumed
δ_v	0.057	assumed
δ_{hb}	0.88	assumed
e	0.92	[3]
α	0.9	assumed
p	0.4	assumed
ω	0.9	assumed
ϕ_h	0.1	[3]
ϕ_{hb}	0.2	assumed
σ_h	0.025	[3]
σ_v	0.025	[3]
ζ	0.86	[3]
C_{hv}	0.18	assumed
η_1	0.1	assumed
η_2	0.2	assumed
η_v	0.07	assumed

5 Conclusion

We have constructed and investigated a mathematical model to evaluate how vaccination affects the spread of dengue disease. First, we have analyzed the model theoretically. According to the theoretical result, when $\mathcal{R}_0 < 1$, the model represents backward bifurcation. The DFE point shows locally asymptotically stable when $\mathcal{R}_0 < 1$. If no re-infection occurs, the DFE point is globally asymptotically stable if $\mathcal{R}_0 < 1$. It is demonstrated that the model has a distinct endemic equilibrium that is locally asymptotically stable whenever the basic reproduction number ($\mathcal{R}_0$) is bigger than one, taking into account the incidence of mass action. Numerical simulation of the model shows that the number of affected individuals decreases as vaccine effectiveness rises. The numerical results also show that the decreasing rate of vaccination waning can lessen the number of infected individuals. Numerical result suggests that the number of infected individuals appears to decline when there is no re-infection. It also suggests that the infected number of humans and mosquitoes decreases as the vaccination rate increases. Our study suggests that it is possible to reduce the disease burden significantly by regulating the transmission probability from humans to mosquitoes. Additionally, our research suggests that the elimination of the dengue disease is possible in the absence of re-infection.

Conflict of interest

The authors have not disclosed conflicts of interest.

Ethical approval

The publication of this paper does not require consent.

References

[1] World Health Organization (2022), Dengue and severe dengue. https://www.who.int/news-room/fact-sheets/detail/dengue-and-severe-dengue. Accessed: 11 November 2022.

[2] Duane J Gubler. Dengue and dengue hemorrhagic fever. *Clinical microbiology reviews*, 11(3):480–496, 1998.

[3] Salisu Mohammed Garba, Abba B Gumel, and MR Abu Bakar. Backward bifurcations in dengue transmission dynamics. *Mathematical biosciences*, 215(1):11–25, 2008.

[4] Neil M Ferguson, Isabel Rodríguez-Barraquer, Ilaria Dorigatti, Luis Mier-y Teran-Romero, Daniel J Laydon, and Derek AT Cummings. Benefits and risks of the sanofi-pasteur dengue vaccine: Modeling optimal deployment. *Science*, 353(6303):1033–1036, 2016.

[5] Laurent Coudeville and Geoff P Garnett. Transmission dynamics of the four dengue serotypes in southern vietnam and the potential impact of vaccination. *PloS one*, 7(12):e51244, 2012.

[6] Isabel Rodriguez-Barraquer, Luis Mier-y Teran-Romero, Ira B Schwartz, Donald S Burke, and Derek AT Cummings. Potential opportunities and perils of imperfect dengue vaccines. *Vaccine*, 32(4):514–520, 2014.

[7] Dennis L Chao, Scott B Halstead, M Elizabeth Halloran, and Ira M Longini Jr. Controlling dengue with vaccines in thailand. *PLoS neglected tropical diseases*, 6(10):e1876, 2012.

[8] NL González Morales, M Núñez-López, J Ramos-Castañeda, and JX Velasco-Hernández. Transmission dynamics of two dengue serotypes with vaccination scenarios. *Mathematical biosciences*, 287:54–71, 2017.

[9] Hamed Al-Sulami, Moustafa El-Shahed, Juan J Nieto, and Wafa Shammakh. On fractional order dengue epidemic model. *Mathematical Problems in Engineering*, 2014, 2014.

[10] Nur'Izzati Hamdan and Adem Kilicman. Analysis of the fractional order dengue transmission model: a case study in malaysia. *Advances in Difference Equations*, 2019(1):1–13, 2019.

[11] Enahoro A Iboi and Abba B Gumel. Mathematical assessment of the role of dengvaxia vaccine on the transmission dynamics of dengue serotypes. *Mathematical biosciences*, 304:25–47, 2018.

[12] Amit Kumar Saha, Chandra Nath Podder, and Ashrafi Meher Niger. Dynamics of novel covid-19 in the presence of co-morbidity. *Infectious Disease Modelling*, 7(2):138–160, 2022.

[13] Pauline Van den Driessche and James Watmough. Reproduction numbers and sub-threshold endemic equilibria for compartmental models of disease transmission. *Mathematical biosciences*, 180(1-2):29–48, 2002.

[14] Odo Diekmann, Johan Andre Peter Heesterbeek, and Johan AJ Metz. On the definition and the computation of the basic reproduction ratio r0 in models for infectious diseases in heterogeneous populations. *Journal of mathematical biology*, 28(4):365–382, 1990.

[15] Joseph P LaSalle. *The stability of dynamical systems*. SIAM, 1976.

[16] Jack Carr. *Applications of centre manifold theory*, volume 35. Springer Science & Business Media, 2012.

[17] Carlos Castillo-Chavez and Baojun Song. Dynamical models of tuberculosis and their applications. *Mathematical Biosciences & Engineering*, 1(2):361, 2004.